Solar energetic particle events in the heliosphere: event on 2013 April 11.

Author: Joan Gratacós i Aurich
Facultat de Física, Universitat de Barcelona, Diagonal 645, 08028 Barcelona, Spain.

Advisor: Maria dels Àngels Aran Sensat

Abstract: Particle radiation during large solar energetic particle (SEP) events may constitute a hazard for space missions. Interplanetary shock waves driven by coronal mass ejections are the largest SEP sources in the inner solar system. We focus on the study of the SEP event on 2013 April 11 by using in-situ particle and solar wind plasma measurements from the Solar Terrestrial Relations Observatory (STEREO) A and B and near-Earth spacecraft. Using the Velocity Dispersion Analysis (VDA) method we estimated the release time of the particles, allowing us to identify the associated parent solar activity, and the distance traveled by the particles. In addition, we determined the energy spectra of the proton intensities at the shock crossing by Earth. Our results agree with predictions from theoretical models.

I. INTRODUCTION

Solar Energetic Particles (SEP) are high-energy particles coming from the Sun. SEPs consist of protons, electrons and heavy ions with energy ranging from a few keV to some GeV/nuc and they are observed in association with solar flares and/or coronal mass ejections (CME).

With the Solar Terrestrial Relations Observatory (STEREO)[1] mission two spacecraft, STEREO-A ("Ahead") and STEREO-B ("Behind) were launched on 26 October 2006 into heliocentric orbits advancing ahead of or trailing behind the Earth, respectively. This offers us the opportunity to make observations of the Sun from multiple locations near 1 AU.

We'll combine the observations on STEREO spacecraft with observations from the Advanced Composition Explorer (ACE)[2], the Solar and Heliospheric Observatory (SOHO)[3] and Wind[4] spacecraft orbiting around the first Sun-Earth Lagrangian point, L1, to study the SEP event on 2013 April 11.

II. OBSERVATIONS

A. Spacecraft Locations and Magnetic Connection

Fig.(1) shows the spatial distribution of the two STEREO and L1 spacecraft from the North ecliptic pole. The green, red and blue dots indicate the locations of the spacecraft orbiting around L1 (we use data from different spacecraft in L1), STEREO-A (A) and STEREO-B (B), respectively. The wide distribution of spacecraft in the inner heliosphere allows us to analize in more detail how the SEP event spreads over a wide range of heliolongitudes.

Table I lists the position of the spacecraft and the solar wind speed around the onset of the particle event. Specifically, in columns 1-2 we list the heliocentric radial distance (R) and the heliographic longitude (Long) of STEREO-A, Near Earth L1 and STEREO-B, respectively. The third column shows the solar wind speed averaged over ten minutes centered at the onset time of the SEP event. In the case of STEREO-A and STEREO-B the solar wind speed was measured by the Plasma and Suprathermal Ion Composition (PLASTIC) instrument whereas at L1 we use data from Wind and ACE (more

Observer	R(AU)	Long	$V_{sw}(km\ s^{-1})$
STEREO-A	0.96	133.4°	537
Near Earth L1	0.99	0.0°	378
STEREO-B	1.02	-141.8°	337

TABLE I: Spacecraft locations and solar wind measurements averaged around the particle event onset time.

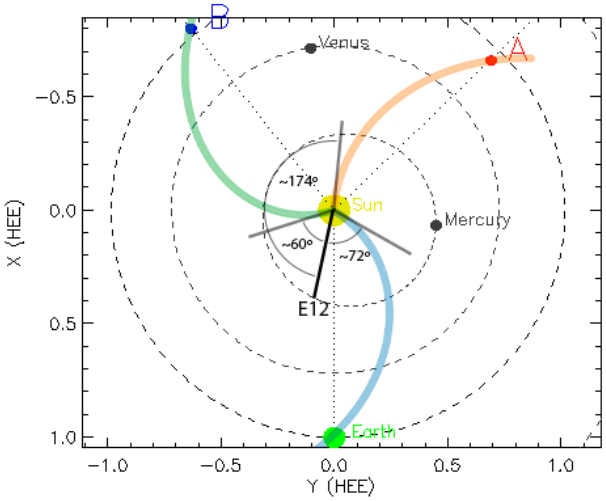

FIG. 1: View from the north ecliptic pole showing the location of STEREO-A (A), STEREO-B (B) and near-Earth observers (Earth) on day 101 of 2013[5]. The nominal Parker spiral magnetic field lines connecting each spacecraft with the Sun are shown. The black line E12 indicates the longitude of the solar parent activity region (E12 as seen from the Earth). The longitudinal distance between the active region and the footpoints of the Interplanetary Magnetic Field (IMF) lines connecting the spacecraft with the Sun are also shown.

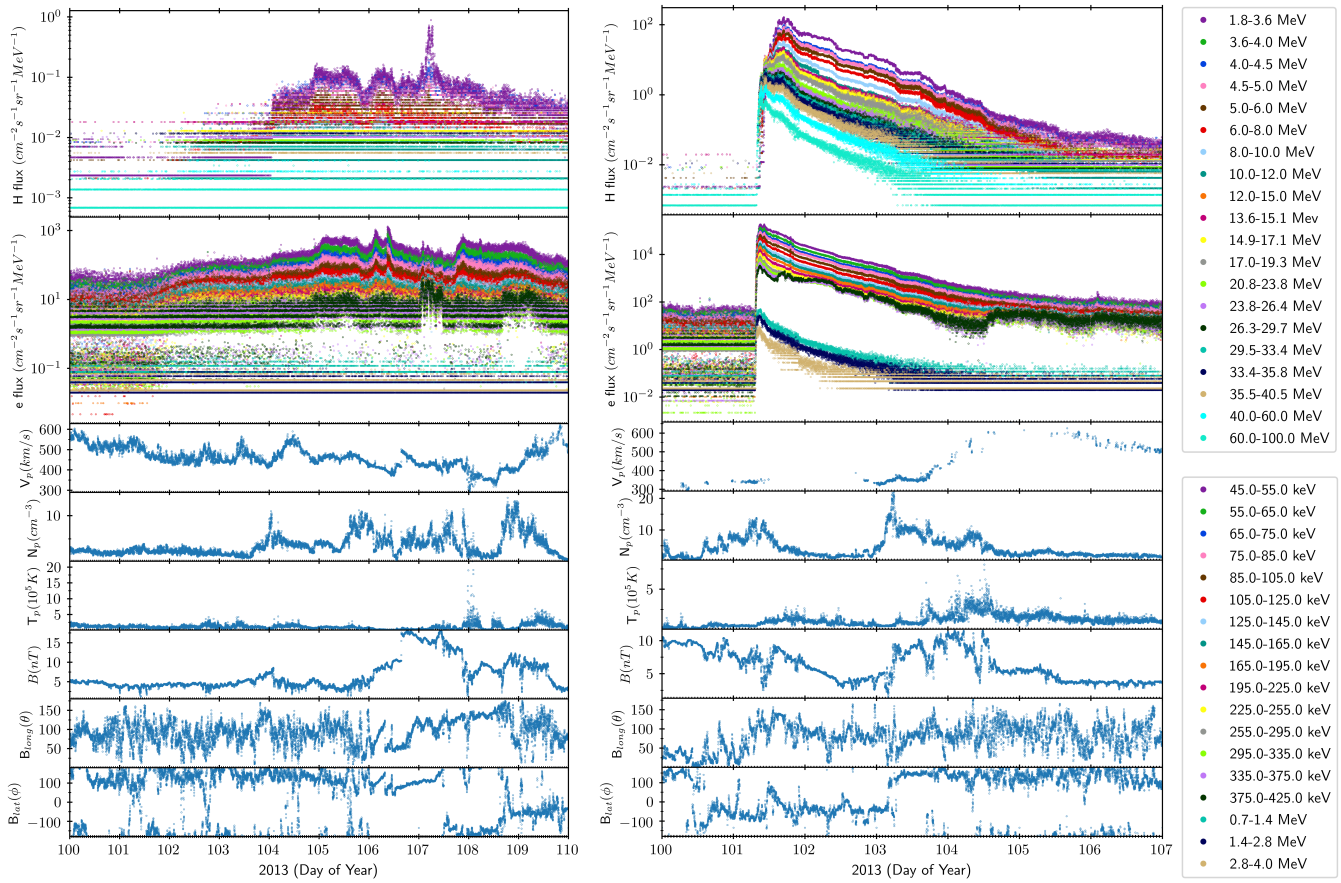

FIG. 2: STEREO spacecrafts observations, STEREO-A (left) and STEREO-B (right). From top to bottom, Intensity-time profiles of protons and electrons, solar wind proton speed V_p, proton number density N_p, proton temperature T_p, total magnetic field B, magnetic field longitude B_{long} and latitude B_{lat}. See section II.B.1 for more information on the data sources.

details in the section II.B). We set the solar wind speed at L1 to the average solar wind speed values from both spacecraft.

Using the Parker model[6] we can approximate the Interplanetary Magnetic Field (IMF) to an Archimedean spiral, therefore, we can calculate the nominal Parker spiral field lines connecting each spacecraft with the Sun (see Fig.(1)) by using:

$$r = V_{sw} \cdot \frac{\varphi - \varphi_0}{\omega_o} + r_0 \tag{1}$$

where r is the radial distance, V_{sw} the solar wind speed, ω_o the solar rotation and φ_0, r_0 are the initial conditions.

We also added in Fig.(1) the longitude of the parent solar activities generating the SEP event (see subsection II.C.2), which is indicated by $E12$ (as seen from the Earth).

To have an idea of how good is the solar region with activity magnetically connected with the spacecraft we calculate the longitudinal distance between the solar region and the footpoint of the spiral IMF lines (Eq. 1) connecting each spacecraft with the Sun. We obtained that $\Delta\psi_{L1} \sim 72°$, $\Delta\psi_{STB} \sim 60°$ and $\Delta\psi_{STA} \sim 174°$, indicating that neither of the spacecraft was well connected with the particles solar source, particularly STEREO-A.

B. Solar Energetic Particles

The data gathered during the SEP event on 2013 April 11 (day of year 101) as seen from the three locations is shown in Fig.(2), Fig.(2) and Fig.(3), respectively for STEREO-A, STEREO-B and L1.

1. *STEREO Data*

In Fig.(2) we show from top to bottom:

- 1 minute averaged intensities. First panel: 1.8 – 15.0 MeV protons measured by the Low-Energy Telescope (LET) and 13.6 – 100 MeV protons measured by the High-Energy Telescope (HET). Second panel: 45.0 – 425.0 keV electrons measured by the Solar Electron and Proton Telescope (SEPT) and 0.7 – 4.0 MeV electrons measured by HET.

- Solar wind data (solar wind proton speed, V_p, proton number density, N_p and proton temperature, T_p, all 1 minute averaged) measured by the PLASTIC instrument.

- Magnetic field data (total magnetic field, B, magnetic field longitude, B_{long}, and latitude, B_{lat}, all 1 minute averaged) measured by the In-situ Measurements of Particles and CME Transients (IMPACT).

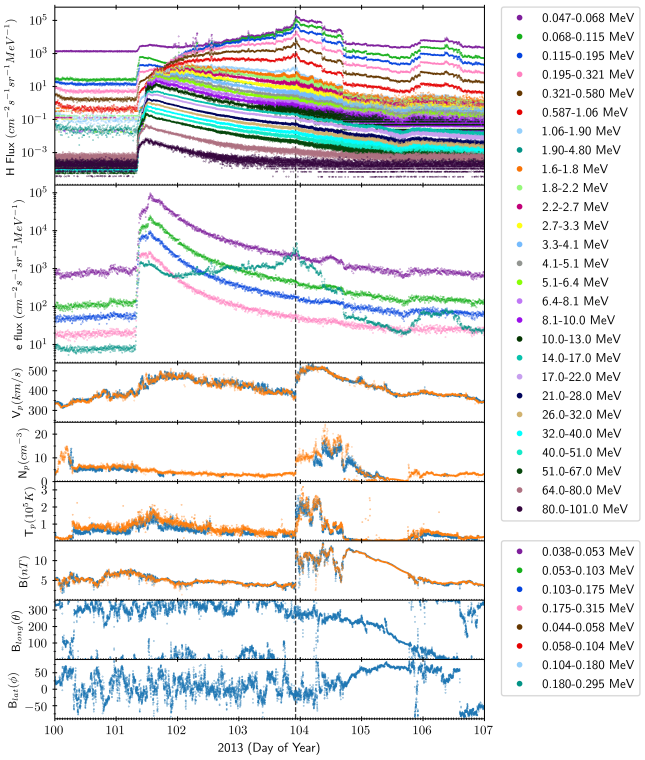

FIG. 3: L1 spacecrafts observations. From top to bottom, Intensity-time profiles of protons and electrons, solar wind proton speed V_p, proton number density N_p, proton temperature T_p, total magnetic field B, magnetic field longitude B_{long} and latitude B_{lat}. See section II.B.2 for more information on the data sources. For the solar wind and magnetic field data we have observations from ACE (blue) and Wind (orange).

2. *Near earth L1 Data*

In Fig.(3) we show from top to bottom:

- 5 minute averaged intensities. First panel: 0.047 – 4.80 MeV protons measured by the Low-Energy Magnetic Spectrometer (LEMS120) detector in the ACE spacecraft and 1.6 – 101.0 MeV protons (1 minute averaged) measured by the Energetic and Relativistic Nuclei and Electron (ERNE) instrument of the SOHO spacecraft. Second panel: 0.038 – 0.315 MeV electrons measured by the Deflected Electrons (DE) detector and 0.044 – 0.295 MeV electrons measured by the Low Energy Foil Spectrometer (LEFS150) detector, both from ACE. Note that LEFS150 energy channels do not only measure electrons but ions too.

- Solar wind data (solar wind proton speed, V_p, proton number density, N_p and proton temperature, T_p, all 64 seconds averaged) was measured by the Solar Wind Electron, Proton, and Alpha Monitor (SWEPAM) instrument in ACE. For these quantities we also used the data measured by the Solar Wind Experiment (SWE) in the Wind spacecraft.

- Magnetic field data (total magnetic field, B, magnetic field longitude, B_{long}, and latitude, B_{lat}, all 64 seconds averaged) was measured by the Magnetic Field Experiment (MAG) instrument in ACE.

C. Data Analysis

In Fig.(2) and (3), we can see an increase on the intensities of both protons and electrons between the days $101 - 102$ at the STEREO-B and L1 locations, respectively. Intensities up to 10^5 [cm^2 s sr MeV]$^{-1}$ for protons and electrons on L1 measurements and up to 10^2 [cm^2 s sr MeV]$^{-1}$ and 10^5 [cm^2 s sr MeV]$^{-1}$ for protons and electrons, respectively, on STEREO-B measurements. This increase in intensity in particles can not be seen in STEREO-A plot (See Fig.(2)), there we can see intensities between 10^{-1} [cm^2 s sr MeV]$^{-1}$ and 10^{-2} [cm^2 s sr MeV]$^{-1}$ for the protons and up to 10^2 [cm^2 s sr MeV]$^{-1}$ for the electrons around the day that the SEP event was measured on L1 and STEREO-B. If we take a look at the spacial distribution of the spacecrafts at the time of the event (See Fig.(1)) we can see that STEREO-A is not magnetically connected or near the solar zone where the solar activity was taking place. We can observe and identify the time of passage of an interplanetary shock by L1 (See Fig.(3), dashed vertical line). This can be identified because of the discontinuities observed in the solar wind plasma and IMF data. The time of passage of the interplanetary shock observed on L1 is on the day of year 103.925129.

1. *Velocity Dispersion Analysis (VDA) method*

The VDA consists of determining the onset times of the particles at every energy channel as function of β^{-1}[7], this way we can estimate both the solar release time and the apparent path length of the particles under the approximation that particles of different energies are released simultaneously at the Sun. The VDA equation at 1 AU can be written as:

$$t_{onset}(E) = t_0 + 8.33\frac{min}{AU} \cdot S \cdot \beta^{-1}(E) \qquad (2)$$

where $t_{onset}(E)$ is the observed onset time in minutes at kinetic energy E, t_0 (min) is the release time from the acceleration site and S (AU) the apparent path length travelled by the particles. The validity of this method is discussed by *Papaioannou et al.* in [7] and references therein.

So, we need to determine for every energy channel the onset time and β^{-1}. To calculate β^{-1} for each energy channel we used the geometric mean of the minimum and maximum values of the energy defining the energy channel. To determine the onset times for each energy channel of the proton intensity measured on L1 and STEREO-B we considered only as valid the first point above 1 sigma from the channel background intensity level that additionally had the next 5 intensities also above the 1 sigma background intensity level.

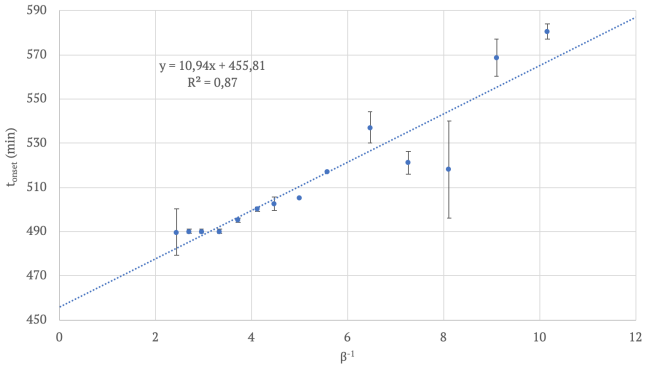

FIG. 4: VDA method for L1 spacecrafts.

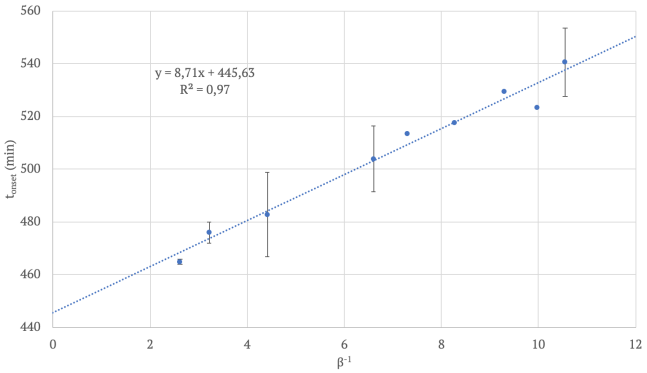

FIG. 5: VDA method for STEREO-B.

Fig.(4) and Fig.(5) show the results of the VDA method applied to the event as observed by the spacecrafts in L1 and STEREO-B, respectively. We can see the release time and apparent distance traveled by the protons using the VDA method in Table II.

We can compare this apparent distance traveled by the protons obtained using the VDA method with the path length along the Archimedean spiral (Parker model) that connects the spacecrafts with the Sun, s, obtained as:

Observer	$t_{release}$ (UT)	S_{VDA} (AU)	S_{Parker} (AU)
Near Earth L1	07:37	1.31	1.15
STEREO-B	07:27	1.05	1.18

TABLE II: The first 2 columns are the VDA method results for each observer considered, the release time $t_{release}$ and the apparent distance traveled by the protons S_{VDA}. The third column is the path length found using the Parker model.

$$s = \frac{1}{2}\frac{V_{sw}}{\omega_\odot}\left[\psi\cdot\sqrt{\psi^2+1}+\ln\left(\psi+\sqrt{\psi^2+1}\right)\right] \qquad (3)$$

with $\psi = \omega_\odot r/V_{sw}$, where $\omega_\odot$ is the Solar rotation and r the radial distance from the Sun to the spacecraft[8]. Results are listed in Table II.

2. *Parent Solar Activities*

Now that we know the approximate release-time of the particles we are able to identify the parent solar activities generating the SEP event. We know that the first particles (earliest onset time) start arriving around 07:45 UT on STEREO-B and 08:10 UT on L1 spacecraft meaning that the solar activity that we are looking for must have taken place prior to these times. We also know by the VDA method (See Table II) that the protons release time from the Sun is around 07:27 - 07:37 UT.

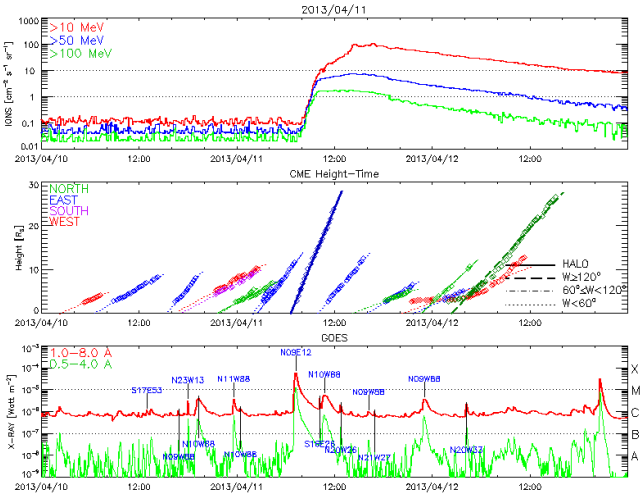

FIG. 6: Ions intensity, CME height over time and the X-ray measured from the Geostationary Operational Environmental Satellite Program (GOES). We can observe a large CME located in N09E12 as seen from the Earth[9].

Now, if we take a look at the SOHO LASCO CME Catalog[9] we find that on April 11 2013 a CME located at N09E12 was observed (See Fig.(6)) at 07:24 UT (First LASCO C2 coronagraph appearance). The time and location (See Fig.(1)) of the CME is consistent with the in-situ observations from STEREO and L1 spacecraft.

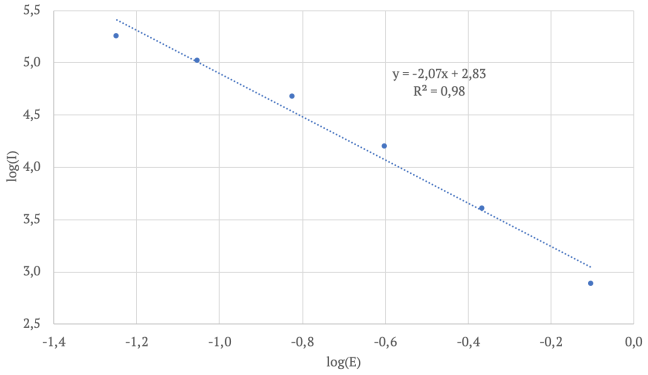

FIG. 7: Energy spectra of the particle intensities at the time of the shock passage by L1

3. Shock Analysis

As we commented earlier, we can see an interplanetary shock passage on L1 plot (See Fig.(3)) as determined from the discontinuities observed on the proton velocity, proton density, temperature and total magnetic field measurements. The smooth rotation observed both in latitude and longitude of the magnetic field after the shock passage indicates that the CME ejecta reached the L1 location. The shock passage takes place on the day of year 103.925129, 22:12 UT on the day 103 (vertical discontinuity line on the Fig.(3)). This result agrees with the data found on the catalog of interplanetary shocks of Wind (day of year 103.925694, 22:13 UT)[10], ACE (day of year 103.958333, ∼23:00 UT)[11] and SOHO (day of year 103.933333, 22:24 UT)[12]. No shock was detected by the two STEREO spacecraft associated with the SEP event.

Fig.(7) shows how the intensity of the particles varies at the shock passage as function of the particle energy. Assuming that the differential Intensity, $I(E)$, can be approximated as a power law with the energy at the shock passage,

$$I(E) = k \cdot E^{-\gamma} \tag{4}$$

we can determine the spectral index, $\gamma = 2.07$, and compare it with the predicted spectral index, q, by the Diffusive Shock Acceleration Theory[13]

$$I \sim E^{(1-q)/2} \qquad with \qquad q = 3r/(r-1) \tag{5}$$

where $r = \frac{n_d}{n_u}$ is the shock compression ratio and n_d and n_u the downstream and upstream plasma proton density, respectively. We obtain $\gamma = (1-q)/2 = 2.25$. Only low energy data has been taken into account since the Diffusive Shock Acceleration Theory diverge for high energies.

III. CONCLUSIONS

Overall the results obtained agree with those predicted by the theory. The VDA method provided a good estimate of the release time and apparent path length of the particles, in agreement with the observed parent solar activity and predicted path length by the Parker model. The energy spectra of the particle intensities at the time of the shock passage obtained from the measurements coincided with the predicted by the Shock Acceleration Theory only at low energy and diverged at high energy as expected.

Acknowledgments

We thank the ACE/EPAM, SWEPAM and MAG instrument teams and the ACE Science Center for providing the ACE data. We acknowledge the use of publicly available data products from WIND/SWE and 3DP, STEREO/HET, LET and SEPT and the CME catalogues from SOHO/LASCO. SOHO is a project of international cooperation between ESA and NASA. We acknowledge also the use of ESA's SEPEM project application server and the use of the Harvard-Smithsonian Interplanetary shock Database maintained by M. L. Stevens and J. C. Kasper. Thanks my advisor, Dr. A. Aran, for her guidance and infinite patience throughout this "Treball de Fi de Grau". Thanks to my family, to my uncle, Dr. J. Aurich Costa, who, although no longer with us, always supported me and continues to inspire me today.

[1] M. L. Kaiser and et al., Space Science Reviews **136**, 5 (2007).
[2] E. Stone and et al., Space Science Reviews **86**, 1 (1998).
[3] V. Domingo and et al., Solar Physics **162**, 1 (1995).
[4] K. Ogilvie and M. Desch, Advances in Space Research **20**, 559 (1997).
[5] URL `http://stereo-ssc.nascom.nasa.gov/cgi-bin/make_where_gif`.
[6] E. N. Parker, The Astrophysical Journal **128**, 664 (1958).
[7] A. Papaioannou and et al., Journal of Space Weather and Space Climate **6**, A42 (2016).
[8] M.-B. Kallenrode, *Space Physics* (Springer Berlin Heidelberg, 2004).
[9] URL `https://cdaw.gsfc.nasa.gov/CME_list/`.
[10] URL `https://www.cfa.harvard.edu/shocks/wi_data`.
[11] URL `http://www.ssg.sr.unh.edu/mag/ace/ACElists/obs_list.html#2013`.
[12] URL `http://umtof.umd.edu/pm/FIGS.HTML`.
[13] L. N. Parker and G. P. Zank, The Astrophysical Journal **757**, 97 (2012).